

Developing a comprehensive Dynamic Model for topologies of DC-AC and AC-AC ZSC converters and design of Impedance Network Controller

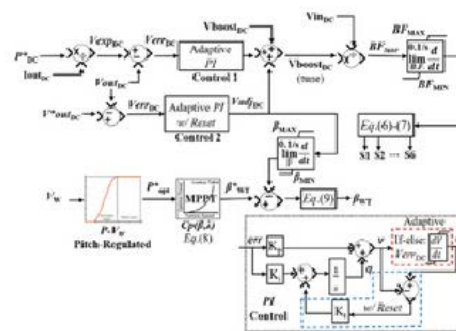
Pravin Ratanlal Choube,* Vikas Kumar Aharwal

Electrical and Electronics Engineering (EX) Department, Dr. APJ Abdul Kalam University Indore (M.P.), India

Received on: 05-Oct-2022, Accepted and Published on: 02-Nov-2022

ABSTRACT

Permanent magnet synchronous generator-powered wind turbines may be connected to the grid using a three-stage power conversion system that consists of an uncontrolled rectifier, a DC voltage source inverter, and a voltage boost converter. A topological modification is made to two intermediate phases by using a quasi-Z source inverter (qZSI). Additionally, a battery is integrated with the qZSI without any additional DC/DC converter. This paper provides an illustration of the use and management of ZSC for large-scale wind turbines with energy storage systems. Depending on the operating circumstances and the battery state-of-charge, qZSI is regulated using a Z-Space Vector Modulation (ZSVM) approach to accomplish maximum power point tracking in the wind turbine, reactive power regulation, and battery charge/discharge. This article provides the modelling and analysis of ac small signals for continuous-conduction mode z source converters (ZSCs). Computer simulation results are utilized to validate the small signal modelling approach after deriving the AC small signal model of ZSC. The ac small signal models are applied in a variety of ways to ZSC design and experimentally verified. Subsequently, a list of expanded MC topologies, including three-level and hybrid MCs, is provided. Three-phase ac-ac buck-type chopper circuits are then explored as a specific instance of matrix converters (MCs). With this, a basis of better values for each of the converter topologies is generated. The performance analysis is examined in light of parasitic resistance, and theoretic computation is used to optimize the system parameter design. This study delivers a thorough evaluation of significant topological advancements in MCIS networks and offers a detailed comparison of key elements.



Topologies
analysis

Keywords: Small signal analysis, state space model, voltage-source converter, z-source converter, control architecture

INTRODUCTION

There is a focus on finding a way to create a more effective buck-boost converter that can transfer AC to AC directly with the least amount of componentry as power converter research expands. Impedance source converter is the idea employed for this. Compared to conventional converters like voltage source (V-source), current source (I-source), and push-pull converters, a Z-source network has the ability to function in shoot-through condition, which helps to increase the output voltage.¹ The three

phase AC to AC Z-source converter simulation work has been completed, and the outcomes are mathematically confirmed. The converter has various restrictions, such as a maximum boost factor of 1.15. With twelve bidirectional switches in an upgraded topology, this restriction is removed. Although better topology requires twice as many switches, the maximum boost factor is still quite high (in our case boost factor obtained is 1.8).² The two converters are thoroughly analysed and contrasted in the thesis work. By using simulation and analytical findings, the voltage sag and swell capabilities of both converters are confirmed.

For both converters' mathematical modelling, state space averaging is used. The concept of single-phase Z-source PWM ac-ac converters (ZSC) was introduced in and offers the following advantages: the output voltage may be boosted or bucked, and it can also be in phase or out of phase with the input voltage. However, they have several serious shortcomings.³⁻⁶

*Corresponding Author: Pravin Choube
Email: pravinchoube2007@gmail.com

Cite as: J. Integr. Sci. Technol., 2023, 11(1), 460.
URN:NBN:sciencein.jist.2023.v11.460

©Authors CC4-NC-ND, ScienceIN ISSN: 2321-4635
http://pubs.thesciencein.org/jist

- The ground between the input and output voltages is not the same.
- A discontinuous current mode is used to operate the input current (DCM).
- Each switch needs an external loss snubber circuit to reduce voltage spikes and offer commutation channels during dead time.

Figure 1 depicts the single-phase trans-Z-source ac-ac converter that is suggested in this work. It has a single inductor L , a connected inductor with two windings (L_1, L_2), two capacitors (C_1, C_2), three bidirectional switches (S_1, S_2 , and S_3), three output filter capacitors (C_1, C_2 , and C), and a load R . In order to create the bidirectional switches, two insulated-gate bipolar transistors (IGBTs) are connected in antiparallel (common back-to-back)⁷. The linked inductor (with two windings L_1, L_2), one inductor L , and two capacitors C_1 and C_2 make up the trans-Z-source network, where $N = n_2/n_1$ is the coupled inductor's turns ratio.

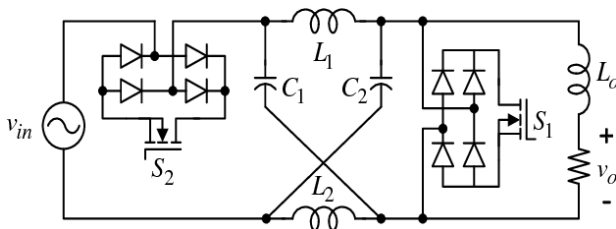


Figure 1: Single-phase trans-Z-source ac to ac converter being proposed

Ac-ac converters with dc-link

The basics of space vector modulation for PWM converters with a dc-link are briefly covered in this section, along with functional equivalent circuit layouts. The PWM inverter stage is taken into account for the V-BBC, whereas the PWM rectifier stage is taken into account for the C-BBC.⁸ As a result, the IMC architecture can be developed by simply coupling the two subsystems together, and the IMC may be modulated by combining and coordinating the modulation schemes of the subsystems.

Voltage DC-Link PWM Inverter

Three bridge legs make up the PWM output stage (inverter) of the V-BBC as seen in Figure 2. Each performs the role of a switch by connecting the output to either the positive or the negative dc-bus, denoted by p and n, respectively.⁹ The output A is linked to p, the outputs B and C are connected to n, and the switching state of the inverter is specified by the expression ($s_1s_2s_3$), where s can be either p or n.

The quasi-ZSC (q-ZSC), which is a derivation of ZSCs and is seen in Figure 3 (a), was introduced by to solve issues such discontinuous input current during boost mode, decreased source stress, and a more straightforward control method. By recommending four topologies for each ZSC and q-ZSC, Specification expanded the applications of ZSCs and q-ZSCs from dc-ac and ac-ac to DC-DC.¹⁰ For both the dc-ac and ac-ac converters, the extension to DC-DC was accomplished by passing the output over a capacitor rather than switch S_2 , as illustrated in Figure 3. (b). There were two classes in each of the DC-DC ZSC and q-ZSC families, and each class had two topologies.

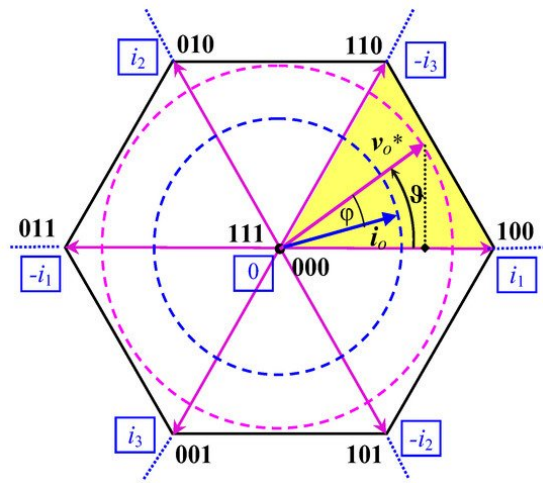


Figure 2 shows the input dc current (framed) for each inverter condition together with the space vector representation of the inverter output voltage ($S_1 S_2 S_3$).

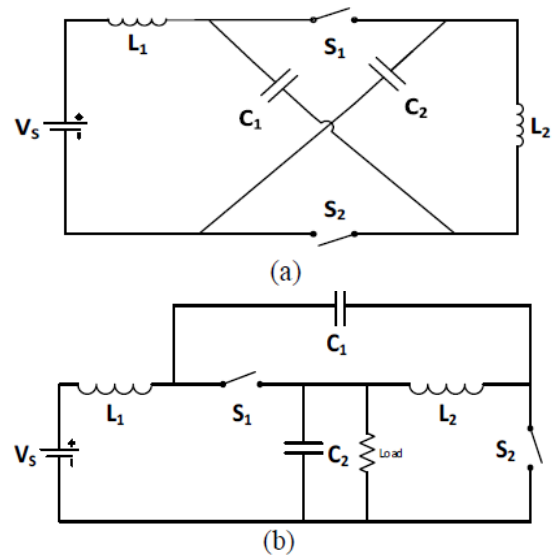


Figure 3. (a) & (b) q-ZSC in general DC-DC q-ZSC

We require appropriate dynamic modelling and analysis in order to create ZSC controllers. It is clear that a precise small signal model of ZSC is required, one that provides design guidance for sizing passive components and an understanding of system constraints while simultaneously offering a complete perspective of system dynamics. However, only a small number of articles have so far added to the dynamic modelling and transient analysis induced by the impedance network that is only found in ZSC.¹¹ An ordinary source dc-ac inverter's ac side is connected to its dc side in order to create a source dc-dc converter, which is then investigated. We will expand the ZSC steady state model to take into account the dynamics that are specifically introduced by the inductors and capacitors that are present in the circuit. As seen in Figure. 4, the load z_1 and an active switch s_2 are connected in parallel in the simplified circuit.

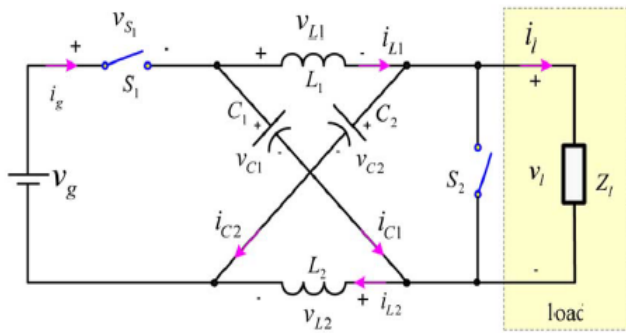


Figure. 4 shows the ZSC's simplified equivalent circuit.

The Evolution of Wind Power Technology

Since lead acid batteries are lighter and smaller than other battery types, researchers have been able to expand their study into using wind turbines to capture solar energy since Camille Faure's creation of lead acid batteries in 1881. In the years that followed, eminent scientists like Professor James Blyth and Charles Brush were able to construct horizontal axis turbines that could charge up the available accumulators and illuminate a single home or piece of property¹². Over 2500 windmills were used to generate 30 MW of peak power in Denmark in the 1890s, thanks to a huge upsurge in wind turbine technology. By the end of the first decade of the 1900s, this statistic transformed into each windmill producing around 25 kW.

PROPOSED CONTROL ARCHITECTURES

The proposed control algorithms for SST-ZSC and VSC (grid-side) operation are discussed below.

Power system Operation with SST-ZSC

The suggested controller for the SST-ZSC, as seen in Figure. 5,

offers droop control integrated with FRT support. It includes two PI-controlled capabilities that operate in parallel¹³: I secondary control, which prevents sub-optimal WECS/MPPT (WT) under normal conditions due to restricted blade pitch elevation, and (ii) main control.

Dynamic Voltage Restorer (DVR)

DVR employs two PI-controlled features (Controls 1 and 2) to provide optimal active power transfer and ride-through voltage. Aag/Swell at ZSC's AC-side via real-time tweaking BF. The boost converter function of the Z-network is enabled by the shoot-through state gating sequence and is shown by the boosting voltage method presented.

- Control 1 adjusts V boost DC based on the referenced active power and available current level at the SST-ZSC output. It also offers correction for voltage sag crises, however exposure to an overvoltage problem during a PMSG interjection of low current is possible¹⁴. As a result, Control 2 acts as an overvoltage compensation by lowering V boost DC to maintain the required amount of DC output from the SST-ZSC.
- Control 2 uses an inbuilt windup-based PI controller (with Reset) to reset state error from overshooting V adjDC.

$$V_{uppreff} = 1 - (BF - 1/2BF) \tag{6}$$

$$V_{bottref} = -1 + (BF - 1/2BF) \tag{6}$$

$$S.T.pulse = \begin{cases} 1 & V_{sw} > V_{uppreff} \\ 1 & V_{sw} < V_{bottref} \\ 0 & \text{otherwise} \end{cases} \tag{7}$$

Volt/Watt as a Supporting Role

The Volt/Watt function works in tandem with the DVR as an additional voltage regulator, using the active power production

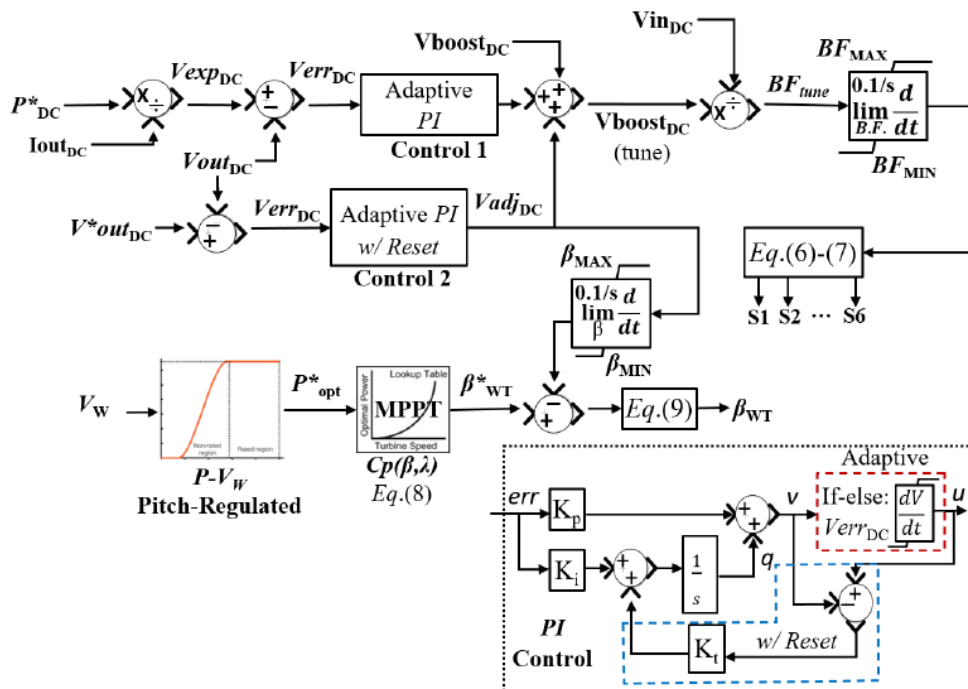


Figure 5. SST-ZSC control architecture for a single cluster of WT and DC collection.

The converter's input line voltages are:

$$\begin{pmatrix} V_{ab} \\ V_{bc} \\ V_{ca} \end{pmatrix} = \begin{pmatrix} V_i.e^{i0} \\ V_i.e^{-i\frac{2\pi}{3}} \\ V_i.e^{i\frac{2\pi}{3}} \end{pmatrix} \quad 4$$

Corresponding Output line Voltages are-

$$\begin{pmatrix} V_{a'b'} \\ V_{b'c'} \\ V_{c'a'} \end{pmatrix} = \begin{pmatrix} V_o.e^{i0} \\ V_o.e^{-i\frac{2\pi}{3}} \\ V_o.e^{i\frac{2\pi}{3}} \end{pmatrix} \quad 5$$

Voltage across Inductors-

$$\begin{pmatrix} V_{L1} \\ V_{L2} \\ V_{L3} \end{pmatrix} = \begin{pmatrix} V_L.e^{i0} \\ V_L.e^{-i\frac{2\pi}{3}} \\ V_L.e^{i\frac{2\pi}{3}} \end{pmatrix} \quad 6$$

Voltage across Capacitors-

$$\begin{pmatrix} V_{C1} \\ V_{Cp} \\ V_{C3} \end{pmatrix} = \begin{pmatrix} V_c.e^{i0} \\ V_c.e^{-i\frac{2\pi}{3}} \\ V_c.e^{i\frac{2\pi}{3}} \end{pmatrix} \quad 7$$

22

Figures 8 and 9, respectively, depict the shoot-through and non-shoot-through states that can exist.²³ The switches Sap, Sbp, and Scp are left on while the switches San, Sbn, and Scn are turned off during non-shoot through time (1-D)T. The switches San, Sbn, and Scn are turned on during shoot-through period DT while the switches Sap, Sbp, and Scp are left off.

Z-source converter for three phase ac to ac with improved

In terms of design and voltage gain, this architecture is significantly different from the prior converter mentioned in this section. This converter has bidirectional switches, an older converter-style Z-network, and injected capacitors. These injected capacitors serve as energy storage devices.^{24,25} These capacitors are added to the Z-energy network's supply during the shoot-through condition in order to charge the Z-source inductors. Consequently, compared to the prior converter, this converter's maximum boost ratio has been increased.

In this setup, eleven bidirectional switches and one bidirectional switch with a diode bridge are employed. The duty cycle may be adjusted to alter the output voltage.

Figure 10: shows the gating signal sequence for this converter. Figure 11: depicts the converter architecture of the suggested converter. Additionally, it has two operating modes: shoot-through mode and non-shoot-through mode. Figures 12: depict the converter's two operational states, respectively.

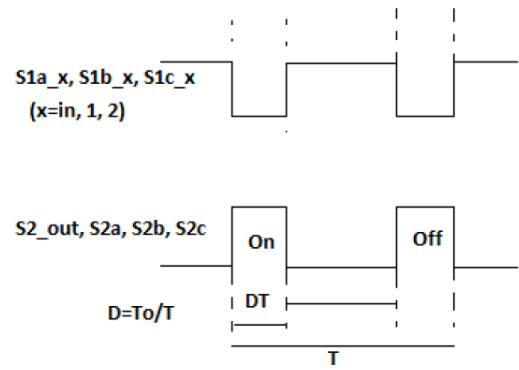


Figure 10: Gating Order

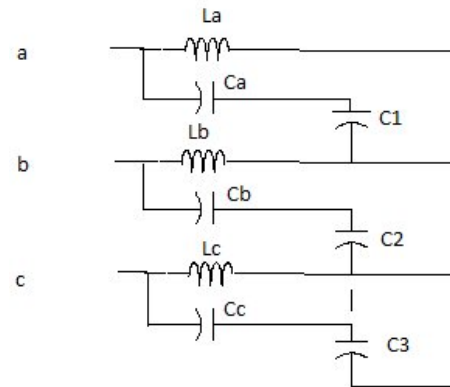


Figure 11: Three Phase AC to AC ZSC's improved architecture

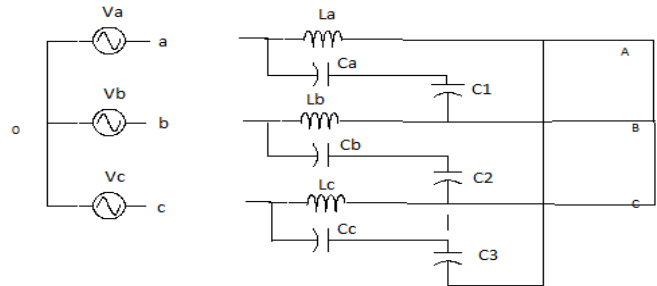


Figure 12: Non-Shoot-Through State

Because the inductors, Z-network capacitors, and injected capacitors all have the identical inductances and capacitances, the three phases of the Z-network are symmetrical. The system's power quality is impacted by the kind of load.^{26,27} The current drawn by linear loads is sinusoidal, preventing waveform distortion. Non-linear loads produce voltage waveform aberrations and current that is not quite sinusoidal. A perfect sine wave is devoid of harmonics.

Control of the 3-phase ac-ac ZSC in closed loop

To produce constant output voltage during voltage sag or swell, closed loop control is required, and for that reason, a PID controller is added as shown in the block diagram below²⁸.

Pid controller: proportional-integral-derivative

A closed loop feedback mechanism called a PID Controller is extensively utilised in industrial control systems²⁹. This controller determines the error value as the difference between the measured

variable and the intended set point. There are three constant constants at play, P, I, and D.

K_p = Proportional Gain	8
K_i = Integral Gain	9
D_k = Derivative Gain	10

The following is a parallel PID representation:

$$C = Kp + \frac{K_i}{s} + \frac{KD^S}{Tf^{S+1}} \quad 11$$

Where Tf is the temporal constant for a first order derivative filter.

For the three-phase ac to ac ZSC, a closed loop control will be designed using the PID Controller. In order to regulate any variations in the input voltage and provide a constant ac output voltage³⁰, The table shown above, which may be used to simulate the closed loop, provides an understanding of the gains' behaviour.

Circuit analysis

Gain derivation and state equations derivation are divided into two categories in this section. For the formulation of the gain and state equations, circuit analysis was performed using ideal and actual circuits³¹, respectively. Two switching modes were used in the analyses with regard to S1, and S2 was complementarily switched with respect to S1 to provide the two operation modes depicted in Figure 13. For modes I and II, the duty ratios are 'D' and '1D', respectively³². While Vg, Ig, RO, and IO are input voltage, input current, load resistance, and load current respectively, C1, C2, L1, and L2 are capacitors and inductors with currents IC1, IC2, IL1, and IL2, and parasitic resistances R1, R2, and r1, respectively.

Gain Derivation

The ideal gain equation for the topology was derived using the ideal circuit of making the simplifying assumption that the parasitic resistances R1, R2 and r1, r2 of the capacitors and inductors are insignificant³³. Mode 1: S1 is ON while S2 is OFF in this mode, as

seen in Figure 13(a). For this mode, the duty ratio is D. Active and reactive AC-side demand are regarded as reference input signals, as shown in Figure 14.

$$P_s(t) = \frac{3}{2} V_{sd}(t) i_d(t), \quad 12$$

$$Q_s(t) = -\frac{3}{2} V_{sq}(t) i_d(t). \quad 13$$

The disparity between a system's input and output in the limit as time approaches infinity is known as steady-state error (i.e., when the response has reached the steady state). The steady-state error will vary depending on the system type and the input type (step, ramp, etc.)³⁴.

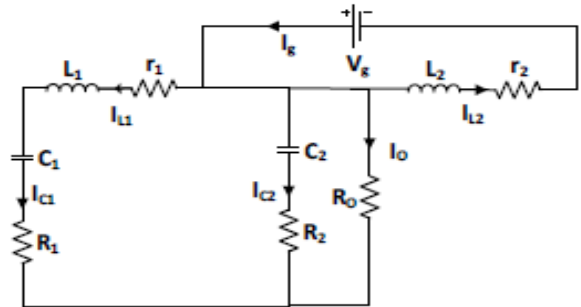


Figure 13. Circuit with parasitic resistances is taken into account

$$VL1 = VO - VC1 \quad 12$$

$$VL2 = Vg \quad 13$$

RESULTS AND DISCUSSIONS

3-phase ZSC analysis without a filter

MATLAB software is used to simulate the ZSI system. Consideration is given to a wind energy conversion system supplying an RL load. To increase the output of WECS to the desired level, the Z-network is utilized.

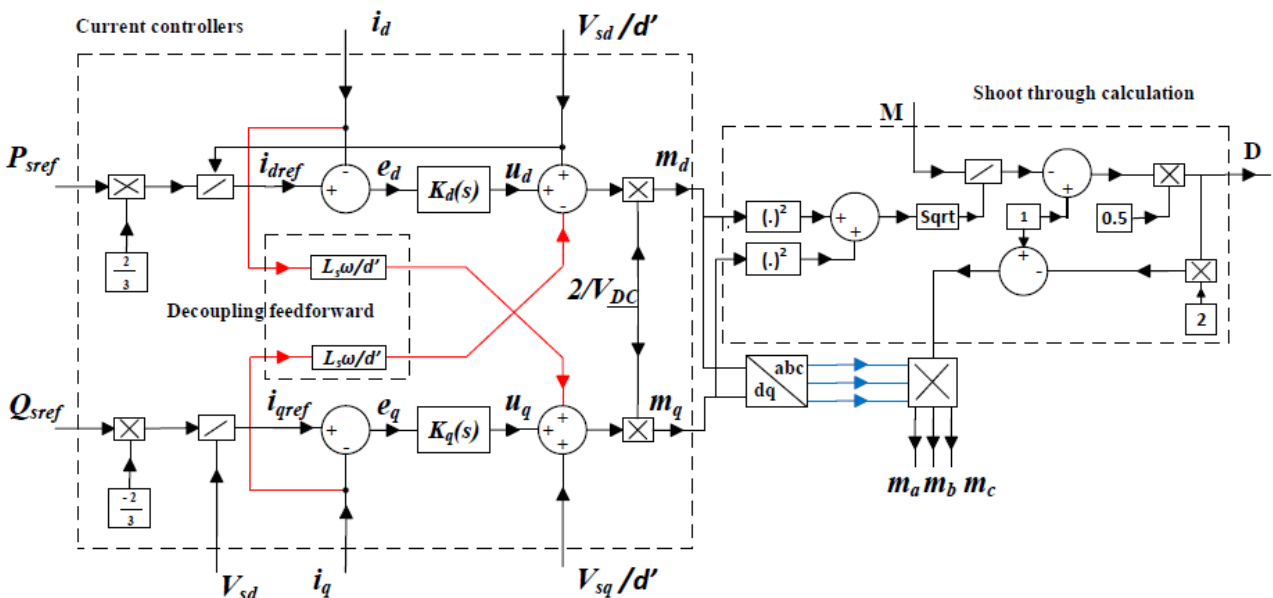


Figure. 14: Control system.

Table 4.1: 3-phase ZSC open loop values with increasing duty cycle

Input voltage(v)	Switching Frequency (kHz)	Duty Cycle	Inductor μ H	Capacitor μ F	Output voltage (V)	THD %age
301	21	0.25	450	10	314.6	191.02
301	21	0.32	450	10	315.6	181.03
301	21	0.35	450	10	318.52	108.28
301	21	0.36	450	10	352.25	107.35

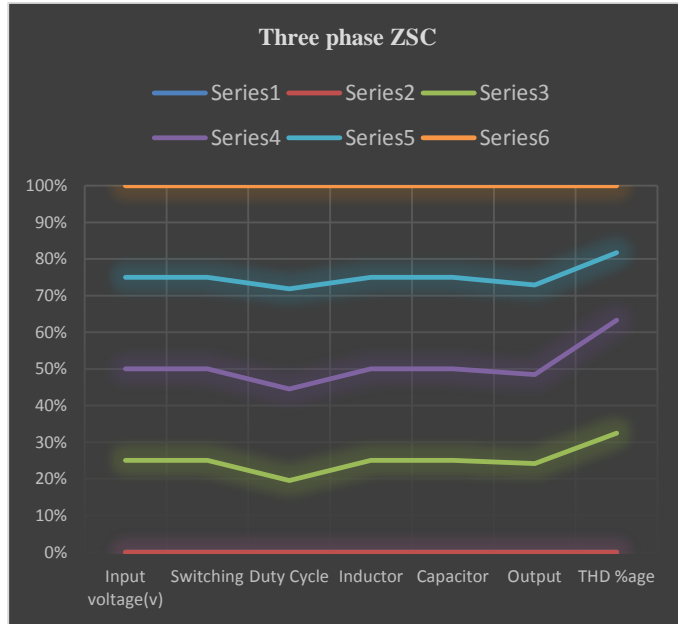


Figure 15. 3-phase ZSC open loop readings with changing duty cycle without a filter

Table 4.2: Open Loop readings of a three-phase ZSC without a filter when the inductance is changed

Input voltage(v)	Switching Frequency (kHz)	Duty Cycle	Inductor μ H	Capacitor μ F	Output voltage (V)	THD %age
301	21	0.7	450 μ H	10	314.6	191.02
301	21	0.7	45 μ H	10	315.6	181.03
301	21	0.7	41 μ H	10	318.52	108.28
301	21	0.7	20 μ H	10	352.25	107.35

After a thorough investigation of the 3-phase ZSC without a filter, we discovered that employing a filter and analysing the behaviour with it is necessary to stabilise the waveform, or to make it sinusoidal. Additionally, the thorough evaluation of 3-phase ZSC with filter is provided.

Results of a three-phase ac to ac ZSC simulation

Figure 17. Displays the three-phase input voltage with a root mean square value of 300V. The following figure shows the peak voltage curve.

The output voltage with impedance network values of 500 H and 10 F, 20 kHz switching rate, and 0.38 duty cycle without the need of a filter. It is evident from Figure 18.'s FFT analysis of the output voltage without a filter that the THD is an unfavourable 193.90 percent. Consequently, the circuit needs a filter to be added.

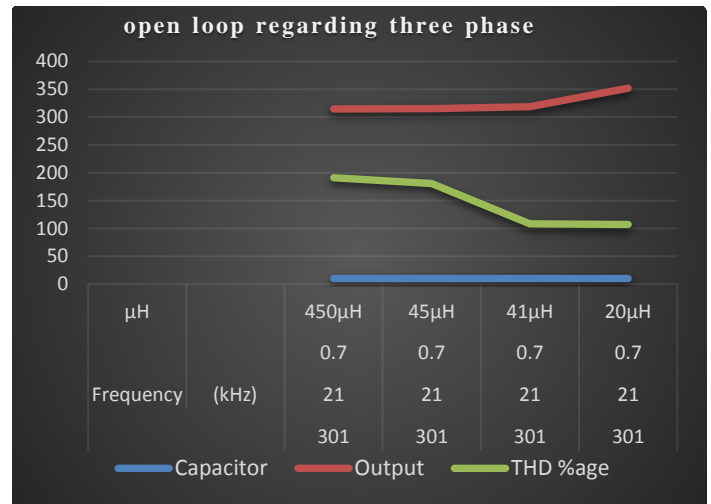


Figure 16. Variable Inductance Open Loop Readings of the 3-phase ZSC without a Filter

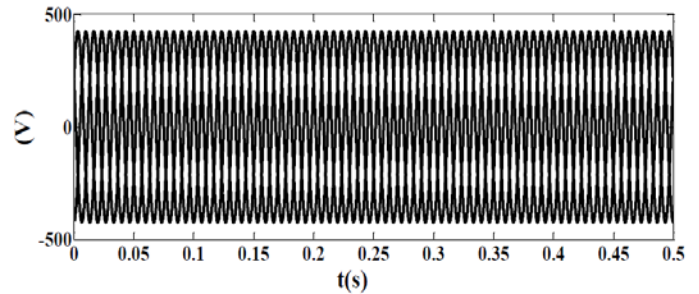


Figure 17: Three phase Balanced Input voltage

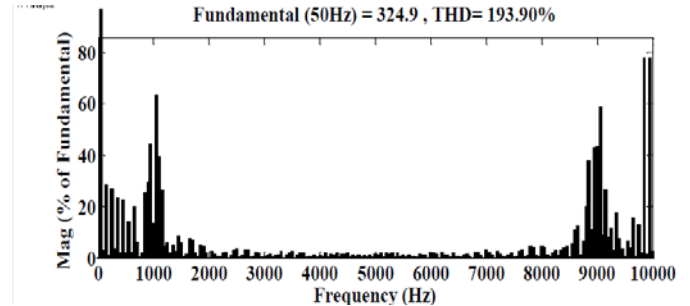


Figure 18: Analysis of the output voltage without a filter's Total Harmonic Distortion (THD)

CONCLUSIONS AND FUTURE SCOPE

In conclusion, A ZSC small signal model that can be connected to the AC grid, and each parameter impact on the system behaviour. Although we now know more about controlling WTs than we did a few years ago, there is still plenty to learn. As a result, this paper concentrates on examining the control of WTs in the open literature to determine what areas of future R&D should be taken into account in order to motivate both business and academics to seek advancements in creating more effective WTs. The literature is evaluated for this purpose, and after that, several questionnaires are sent to industry experts to complete in accordance with the issue's importance. Here, a practical overview is given to explain and look at the concerns that should be prioritised to produce better and more effective WTs. Some popular controllers and contemporary examples are discussed in the current article. Power electronic-

based devices such DGs, dynamic reaction of the frequency converter and voltage stability is undoubtedly crucial. Then again important benefits of ZSC that are highlighted in it also features a quicker and smoother dynamic than earlier efforts. Lower order harmonics at the AC port in response and, in contrast, the capacity to reduce the short circuit current designers with VSC that serve as important criterion. Engineering professionals choose the best converter. This converter's stability margin is decent acceptable. Consequently, it can be a suitable alternative for future high-power applications.

- A buck-boost converter may be created using a three-phase ac to ac Z-source converter.
- Three phase ac to ac converters with two different topologies have been compared. The better topology solves the drawback of the earlier one, which was that it could only increase voltage by a maximum of 15%.
- The equipment can be protected against voltage swell and sag by either converter, but the upgraded topology has better capabilities.
- Both input voltage fluctuation and load variation are handled by the closed loop controller.
- Simulation analysis shows that the converter's filter has an effect on the magnitude of the voltage.

REFERENCES

1. A. Chaudhuri, R. Datta, M.P. Kumar, J.P. Davim, S. Pramanik. Energy Conversion Strategies for Wind Energy System: Electrical, Mechanical and Material Aspects. *Materials* **2022**, 15 (3), 1–34.
2. A. Yadav, S. Chandra, M. Bajaj, et al. A Topological Advancement Review of Magnetically Coupled Impedance Source Network Configurations. *Sustainability* **2022**, 14 (5), 1–17.
3. J. Divya Navamani, A. Lavanya, D. Almakhles, M. Jagabar Sathik. A review on segregation of various high gain converter configurations for distributed energy sources. *Alexandria Engin. J.* **2022**, 61 (1), 675–700.
4. P.R. Choube, V.K. Aharwal. Development of suitable closed loop system for effective wind power control using different ZSC topologies and different switching techniques. *J. Integr. Sci. Technol.* **2022**, 10(2), 156–67.
5. P.R. Choube, V.K. Aharwal. Evaluation of Z-Source Inverter Topologies for Power Conditioning Unit for DC Power Supply Systems. *J. Integr. Sci. Techn.* **2022**, 10 (3), 209–214.
6. C. Gupta, V.K. Aharwal. Optimizing the performance of Triple Input DC-DC converter in an Integrated System. *J. Integr. Sci. Technol.* **2022**, 10 (3), 215–220.
7. B. Sun, Z. Chen, C. Gao, et al. A Power Decoupling Control for Wind Power Converter Based on Series-Connected MMC and Open-Winding PMSG. *IEEE Trans. Industrial Electronics* **2022**, 69 (8), 8091–8101.
8. Y. Wang, Y. Guan, O.B. Fosso, et al. An Input-Voltage-Sharing Control Strategy of Input-Series-Output-Parallel Isolated Bidirectional DC/DC Converter for DC Distribution Network. *IEEE Transactions on Power Electronics* **2022**, 37 (2), 1592–1604.
9. J. Sun, M. Xu, M. Cespedes, M. Kauffman. Data Center Power System Stability - Part I: Power Supply Impedance Modeling. *CSEE J. Power and Energy Systems* **2022**, 8 (2), 403–419.
10. J. Sun, S. Wang, J. Wang, L.M. Tolbert. Dynamic Model and Converter-Based Emulator of a Data Center Power Distribution System. *IEEE Transactions on Power Electronics* **2022**, 37 (7), 8420–8432.
11. S.K. Ghosh, T.K. Roy, M.A.H. Pramanik, M.A. Mahmud. Design of nonlinear backstepping double-integral sliding mode controllers to stabilize the dc-bus voltage for dc-dc converters feeding cpls. *Energies* **2021**, 14 (20), 6753.
12. M.B.M.S. Ramadan, R.T. Naayagi. Impedance Source Inverter Wind Turbine and DC Collection System: Fault Ride-Through Analysis. *3rd Int. Conf. Energy, Power and Environment: Towards Clean Energy Technologies, ICEPE 2020* **2021**, 2–7.
13. N. Charrak. Investigation on Multi-Phase Z source. Doctoral dissertation, Université de Djelfa-Ziane Achour. **2021**.
14. E.P.P. Soares-Ramos, L. De Oliveira-Assis, R. Sarrias-Mena, et al. Large-Scale Wind Turbine with Quasi-Z-Source Inverter and Battery. *Proceedings of the IEEE Int. Conf. Industrial Technology* **2021**, 2021-March, 403–408.
15. W. Liu, Modeling and Control of Impedance Source Converters for Grid-Connected PV Systems. Ph.D. Thesis, Aalborg Universitet. **2021**.
16. X. Wu, J. Wang, Y. Zhang, et al. Review of DC-DC Converter Topologies Based on Impedance Network with Wide Input Voltage Range and High Gain for Fuel Cell Vehicles. *Automotive Innovation* **2021**, 4 (4), 351–372.
17. M.A. Awal, I. Husain. Transient Stability Assessment for Current-Constrained and Current-Unconstrained Fault Ride through in Virtual Oscillator-Controlled Converters. *IEEE J. Emerging and Selected Topics in Power Electronics* **2021**, 9 (6), 6935–6946.
18. S. Mungkasi. An order verification method for truncated asymptotic expansion solutions to initial value problems. *Alexandria Engineering J.* **2022**, 61 (1), 175–184.
19. L. de Oliveira-Assis, P. García-Triviño, E.P.P. Soares-Ramos, et al. Optimal energy management system using biogeography based optimization for grid-connected MVDC microgrid with photovoltaic, hydrogen system, electric vehicles and Z-source converters. *Energy Conversion and Management* **2021**, 248.
20. Z.H. Khan, T.A. Gulliver, W. Imran, et al. A macroscopic traffic model based on relaxation time. *Alexandria Engineering J.* **2022**, 61 (1), 585–596.
21. G. Zhang, N. Jin, S.S. Yu, Y. Zhang. An X-shaped-switching-network high-step-up converter for grid integration of renewable energy sources. *AEU - Int. J. Electronics and Commun.* **2021**, 136, 153776.
22. K.V. Kkuni, S. Mohan, G. Yang, W. Xu. Comparative assessment of typical controlrealizations of grid forming converters based on their voltage source behaviour. *arXiv preprint arXiv:2106.10048* **2021**, 1–22.
23. G. Li, Y. Chen, A. Luo, Y. Wang. An inertia phase locked loop for suppressing sub-synchronous resonance of renewable energy generation system under weak grid. *IEEE Transactions on Power Systems* **2021**, 36 (5), 4621–4631.
24. T. Abedin, M.S.H. Lipu, M.A. Hannan, et al. Dynamic modeling of hvdc for power system stability assessment: A review, issues, and recommendations. *Energies* **2021**, 14 (16).
25. R. Zhou, J. Jin, Y. Cui, et al. Agricultural drought vulnerability assessment and diagnosis based on entropy fuzzy pattern recognition and subtraction set pair potential. *Alexandria Engineering J.* **2022**, 61 (1), 51–63.
26. M. Ado, A. Jusoh, T. Sutikno, M.H. Muda, Z.A. Arfeen. Dual output DC-DC quasi impedance source converter. *Int. J. Electrical and Computer Engineering* **2020**, 10 (4), 3988–3998.
27. I. Talib, F. Jarad, M.U. Mirza, A. Nawaz, M.B. Riaz. A generalized operational matrix of mixed partial derivative terms with applications to multi-order fractional partial differential equations. *Alexandria Engineering J.* **2022**, 61 (1), 135–145.
28. E. Bonyah, M.L. Juga, C.W. Chukwu, Fatmawati. A fractional order dengue fever model in the context of protected travelers. *Alexandria Engineering Journal* **2022**, 61 (1), 927–936.
29. A. Shourangiz-Haghighi, M. Diazd, Y. Zhang, et al. Developing More Efficient Wind Turbines: A Survey of Control Challenges and Opportunities. *IEEE Industrial Electronics Magazine* **2020**, 14 (4), 53–64.
30. V.G.R. Kummara, K. Zeb, A. Muthusamy, et al. A comprehensive review of DC-DC converter topologies and modulation strategies with recent advances in solar photovoltaic systems. *Electronics*, **2019**, 9(1), 31.
31. M. Ado, A. Jusoh, A.U. Mutawakkil, T. Sutikno. Dynamic model of a DC-DC quasi-Z-source converter (q-ZSC). *Int. J. Electrical and Computer Engineering* **2019**, 9 (3), 1585–1597.
32. J.W. Kolar, T. Friedli, J. Rodriguez, P.W. Wheeler. Review of Three-Phase PWM AC – AC Converter Topologies. *IEEE Transactions on Industrial Electronics* **2011**, 58 (11), 4988–5006.
33. M. Ado, A. Jusoh, T. Sutikno. Extended family of DC-DC quasi-Z-source converters. *Int. J. Electrical Computer Engineering* **2019**, 9 (6), 4540–4555.
34. L. He, J. Nai, J. Zhang. Single-phase safe-commutation trans-Z-source AC-AC converter with continuous input current. *IEEE Transactions on Industrial Electronics*, **2017**, 65(6), 5135-5145.